Journal of Theoretical Biology 317 (2013) 55–61

Contents lists available at SciVerse ScienceDirect

Journal of Theoretical Biology

journal homepage: www.elsevier.com/locate/yjtbi

Density thresholds for Mopeia virus invasion and persistence in its host *Mastomys natalensis*

J. Goyens [a,*], J. Reijniers [a], B. Borremans [a], H. Leirs [a,b]

[a] University of Antwerp, Evolutionary Ecology Group, Groenenborgerlaan 171, B-2020 Antwerpen, Belgium
[b] Danish Pest Infestation Laboratory, University of Aarhus, Faculty of Agricultural Sciences, Department of Agro-ecology, Forsøgsvej 1, DK-4200 Slagelse, Denmark

HIGHLIGHTS

- We built a spatially explicit and individual-based SEIR model of Mopeia virus.
- Sharp density thresholds are observed for persistence, not invasion.
- Host dispersal is important for the spread and persistence of the infection.
- In the year following invasion, herd immunity can hinder persistence.
- The model is most sensitive to transmission rate and infectious period.

ARTICLE INFO

Article history:
Received 30 January 2012
Received in revised form
28 September 2012
Accepted 29 September 2012
Available online 4 October 2012

Keywords:
Arenavirus
Infectious disease
Stochastic model
SEIR
Herd immunity

ABSTRACT

Well-established theoretical models predict host density thresholds for invasion and persistence of parasites with a density-dependent transmission. Studying such thresholds in reality, however, is not obvious because it requires long-term data for several fluctuating populations of different size. We developed a spatially explicit and individual-based SEIR model of Mopeia virus in multimammate mice *Mastomys natalensis*. This is an interesting model system for studying abundance thresholds because the host is the most common African rodent, populations fluctuate considerably and the virus is closely related to Lassa virus but non-pathogenic to humans so can be studied safely in the field. The simulations show that, while host density clearly is important, sharp thresholds are only to be expected for persistence (and not for invasion), since at short time-spans (as during invasion), stochasticity is determining. Besides host density, also the spatial extent of the host population is important. We observe the repeated local occurrence of herd immunity, leading to a decrease in transmission of the virus, while even a limited amount of dispersal can have a strong influence in spreading and re-igniting the transmission. The model is most sensitive to the duration of the infectious stage, the size of the home range and the transmission coefficient, so these are important factors to determine experimentally in the future.

1. Introduction

The driving force behind all infectious diseases is the transmission of parasites from an infected to a susceptible host (Begon et al., 2002). Sometimes direct contact between individuals is required for transmission, but also indirect contact (e.g. through contaminated excreta) can be sufficient. When the contact rate between hosts is constant, for example due to social rules, the transmission is called 'frequency-dependent'. When the contact rate between hosts increases at higher population densities, the transmission rate is 'density-dependent' (Begon et al., 2002; Lloyd-Smith et al., 2004, 2005; Keeling and Rohani, 2007). In the latter case, theoretical models predict that there exists a host abundance threshold, which is the minimum number of host individuals needed for an infection to spread in a population (Kermack and McKendrick, 1927).

The nature of the abundance threshold depends on the situation, and two different thresholds can be discerned (Deredec and Courchamp, 2003; Lloyd-Smith et al., 2005). When an infectious agent enters a naive (uninfected and wholly susceptible) population, the density of hosts should be high enough to ensure sufficient contacts between individuals during which transmission can take place. This is then called an invasion threshold (Deredec and

* Corresponding author. Current address: University of Antwerp, Laboratory for Functional Morphology, Universiteitsplein 1, B-2610 Antwerpen, Belgium. Tel.: +32 3 265 2260.
E-mail addresses: jana.goyens@ua.ac.be (J. Goyens), jonas.reijniers@ua.ac.be (J. Reijniers), benny.borremans@ua.ac.be (B. Borremans), herwig.leirs@ua.ac.be (H. Leirs).

0022-5193/$ - see front matter © 2012 Elsevier Ltd. All rights reserved.
http://dx.doi.org/10.1016/j.jtbi.2012.09.039

Courchamp, 2003; Lloyd-Smith et al., 2005). When an infection is already present in a population, persistence will depend on the capacity of the population to produce a sufficient supply of new susceptible individuals, through birth or immigration. Thus, while invasion and persistence thresholds are part of the same concept, they are not completely equivalent (Deredec and Courchamp, 2003; Lloyd-Smith et al., 2005).

In general, human populations do not vary extensively in time, and consequently, these concepts have been hard to demonstrate for human infections (but see critical community size in measles, Bartlett, 1960; Nåsell, 2005; also mass vaccinations aiming at herd immunity are based on the same principle). However, wildlife populations often exhibit larger fluctuations, in which case such thresholds are more likely to be crossed. Periods during which a pathogen can invade, spread and (temporarily) persist, are then interrupted by periods below the threshold, when the pathogen can no longer invade or persist. One example of such an abundance threshold over time can be seen for plague in populations of great gerbils in Kazakhstan (Davis et al., 2004).

In this paper, we study the infection dynamics of Mopeia virus (an East African arenavirus) in its natural host the multimammate mouse (*Mastomys natalensis*). This is an interesting model system for studying epidemiological abundance thresholds, for several reasons. Mopeia virus transmission is thought to be density dependent because the home ranges of its host overlap more at higher densities (Monadjem and Perrin, 1998), so the existence of an abundance threshold is to be expected. Next, because the host populations exhibit large (seasonal as well as interannual) population fluctuations (ranging from <50 to 600 animals per hectare in the same year Leirs et al., 1997), this threshold is likely to be crossed regularly. Additionally, *M. natalensis* is one of the most common African small mammals and an agricultural pest, and as such, its ecology and demography have been studied extensively (e.g. Leirs, 1994). Last, because Mopeia virus is not known to cause disease in humans but is very closely related to the West African Lassa virus (which causes Lassa fever, a severe hemorrhagic fever in humans and thus difficult to study, but with the same rodent species as natural host), insights into Mopeia virus transmission can be used to better understand Lassa virus epidemiology.

As a first step in studying Mopeia virus dynamics, we here develop an individual-based SEIR model to simulate the infection dynamics. Using the current best estimates of the model parameters, the model should be able to tell us if abundance thresholds are to be expected and in which situations. Moreover, as not all epidemiological parameters have been determined experimentally, this model can give important insights into the relative importance of the different transmission parameters in the infection dynamics. This should provide a more reliable foundation for future studies and a guide as to which parameters are more important to be determined experimentally and to what detail.

2. Model

To simulate the spread of Mopeia virus infection, we built an individual-based spatially explicit SEIR model, taking into account demography, spatial behaviour of the host, and the infection dynamics of Mopeia virus. Birth, death, dispersal and the transitions between infection stages are applied stochastically on individual hosts, because the host population can be small and/or the numbers of infected mice can be low. We did not alter the demographic and spatial components after infection, because no overt signs of disease were observed after Lassa virus infection (Walker et al., 1975; Günther and Lenz, 2004).

2.1. Demographic component

In the course of a year, *M. natalensis* shows strong population size fluctuations. These are due to seasonal reproduction, which is driven by seasonal rainfall (May until July, Leirs et al., 1997). Because it is to be expected that the population density greatly influences the infection transmission, it is important to include demography in the model. We include two maturation stages: juvenile and adult, which are governed by the demographic processes of birth, maturation and death, as outlined below.

Birth: Reproduction rates (v) between 0.044 and 0.3 births per day per adult have been observed (Leirs, 1994; Leirs et al., 1997). In the model, an average birth rate of 0.172 mice/day is assumed during the breeding season. Only female adults can reproduce, and the birth rate is adjusted accordingly ($v=0.344$ mice/day). Empirical data have shown that litter sizes are smaller at high densities (Leirs et al., 1997). This density dependence was found to differ between seasons (in reality, some litters are raised outside the breeding season), and is smallest in the reproductive season. For this reason, we do not include this in the model. The litter size was taken to be 11, i.e., the average litter size in Morogoro (11.31, in Leirs, 1994). At birth, the pups are randomly assigned to a sex.

Maturation: In years with a normal rain pattern, the juveniles undergo a long period of reduced growth in the dry season. Because of this, reproduction is postponed until the next breeding season (Leirs et al., 1993, 1997). This delay in the maturation is included in the model.

Death: The mortality of *M. natalensis* was found to be density dependent: at low population densities (below a critical density of 150 mice/ha), the mortality rate (μ) was measured to be 0.0104 mice/day; at higher population densities (well above 150 mice/ha), μ was found to be 0.0158 mice/day (Leirs et al., 1997). In the model, the density-dependent mortality was implemented in the same way, using the above mortality rates, separated by a critical density C. Due to the increased mortality above the critical density C, the population density will level off quickly above C and for this reason, in the following, we refer to C as the carrying capacity. This method, albeit unconventional, has the advantage that it mimics the empirical data and that it allows to change the population density using a single parameter C. Different habitats can sustain a different number of mice (depending on food availability, soil type, etc., Borremans et al., 2011), and therefore, in the analysis we will not restrict ourselves to the experimentally measured $C=150$ mice/ha and vary C to study the effect of the carrying capacity of the habitat on the infection dynamics. It proved necessary though, to lower the overall mortality by 30% in order to adjust it to the birth rate, so that the population would not fade out. This is due to the fact that the experimentally determined mortality rates were somewhat overestimated, because they were inferred from the mice's presence in an open grid of 1 ha, not taking into account emigration as a possible alternative to death when animals disappear from the grid.

2.2. Spatial component

The *M. natalensis* individuals in the simulations are bound to their home burrow. While foraging, an individual moves through the landscape around his burrow, covering only a small area of the total focus. This home range size was estimated by Leirs (590 m^2 for females and 598 m^2 for males, Leirs, 1994; Leirs et al., 1996) and Monadjem and Perrin (1998, 652 m^2 for females and 718 m^2 for males). Due to this limited home range, contacts between individuals cannot be described using a random mixing

assumption and it is necessary to include the spatial behaviour of multimammate mice in the model.

In the model, every animal has a home burrow, represented by coordinates on a grid that remain fixed most of the year. We model the daily movement of an individual by a diffusive motion in a circular symmetric quadratic attractive potential, centered round its burrow (Abramson et al., 2006). The solution of the diffusive equation in such a potential is a two-dimensional Gauss distribution (Worton, 1989; Seaman and Powell, 1996; Abramson et al., 2006; Wilkinson, 2006)

$$K_a(\vec{r}) = K(\vec{r} - \vec{r}_a) \tag{1}$$

$$K_a(\vec{r}) = \frac{1}{2\pi\sigma^2}\exp\left[-\frac{(\|\vec{r} - \vec{r}_a\|)^2}{2\sigma^2}\right] \tag{2}$$

$$K_a(\vec{r}) = \frac{1}{\sqrt{2\pi}\sigma} f(\|\vec{r} - \vec{r}_a\|; 0, \sigma^2), \tag{3}$$

which can be, due to isotropy, reduced to a radial one-dimensional Gaussian function with zero mean and variance σ^2. The kernel $K_a(\vec{r})$ is the probability density function (pdf), and expresses the probability that an individual with a burrow at position $\vec{r}_a$ is at a certain position $\vec{r}$. In the model, the width of the kernel was chosen to be $\sigma = 4.77\ m$, so that the home range covers 95% of all movements (Shchipanov and Lyapina, 2008). Note that we assume that all animals, irrespective of their age or sex, have the same home range size (Leirs, 1994; Leirs et al., 1996; Monadjem and Perrin, 1998).

When a female adult in the model gives birth, its offspring adopts the coordinates of its mother. The mice stay in the same burrow until the dispersal season starts. From October until December, the mice start searching for new places to settle. In this period, monthly 24% of the population displaces its home range (Leirs, 1994) by an average distance of 300 m (dispersal is not clearly sexbiased in *M. natalensis*, Leirs, 1994; Van Hooft et al., 2008). In the model this displacement was included by randomly selecting dispersing animals, which were shifted a fixed distance of 300 m in a random direction. When an individual ends up outside the grid, it is placed on the grid as if it underwent an elastic collision with the edge of the grid. By doing so, the modeled grid represents a closed system of, for example, a patch of suitable habitat in an unsuitable matrix.

2.3. Infection component

In our model, we discern four different stages of infection: susceptible (S), exposed (E), infected (I), and recovered (R). In the following, we describe the serial transition along the chain of different infection stages.

S→E

The transmission mechanisms of Mopeia virus in *M. natalensis* are not fully known yet, but some information can be obtained from related viruses. Direct transmission (e.g. by sexual contacts, grooming or fights) is an important transmission mode for many arenaviruses (Jay et al., 2005), and it is likely that Lassa virus (which is closely related to Mopeia virus) can be passed on indirectly by aerosols (in urine, saliva or faeces) (Walker et al., 1975; Peters et al., 1987). Some preliminary infection experiments were conducted (unpublished data), and they showed that animals can indeed become infected through indirect transmission with contaminated environment. So, both indirect and direct transmission are possible routes, but their relative importance is still unknown.

However, this will turn out to be of little importance for modeling the infection dynamics, as it will prove out that they can be modeled in the same way, because of the short survival time of the virus outside the host. But first we focus on modeling transmission through direct contact.

The rate at which a susceptible mouse j becomes infected by an infectious mouse i is proportional to their contact rate. *M. natalensis* is thought to be nonterritorial (Veenstra, 1957; Leirs et al., 1996), so the overlap of home ranges will increase with density (Monadjem and Perrin, 1998). This overlap will determine to what extent neighbouring animals interact with each other. Hence, the contact rate, in turn, is proportional to the spatial overlap $O(i,j)$ between the pdf's of both animals, which can be rewritten as

$$O(i,j) = \int\int K_i(\vec{r}) K_j(\vec{r})\, d\vec{r} \tag{4}$$

$$O(i,j) = \frac{1}{2\sqrt{\pi}\sigma} f(\|\vec{r}_i - \vec{r}_j\|; 0, 2\sigma^2), \tag{5}$$

since the convolution of two Gaussian functions is again a Gaussian function, but now with summed variance. As the contact rate is proportional to the spatial overlap, the contact rate equals $cO(i,j)$, with c a constant rate. The rate ψ at which a susceptible individual becomes infected, is then given by

$$\psi(j) = v\sum_i cO(i,j) = \beta\sum_i O(i,j), \tag{6}$$

where the sum is over all infected animals i, and where v entails the probability for successful virus transmission during an encounter. Both unknown parameters v and c can be contained within a single transmission coefficient $\beta = vc$.

For indirect transmission, the virus passes via contaminated ground. Once an infected animal becomes infectious, it starts shedding virus into its surroundings, and, as time goes by, the amount of virus in its surroundings will increase until it reaches a plateau. Indeed, the virus has a rather short survival time (the viral load of Lassa virus decreases by 90% in 58.2 h; Sagripanti et al., 2010), and decays in the soil, leading to a very quick saturation of the contamination load (Fig. 1). Because of this rather short virus survival time, the 'memory' of the ground is rather short compared to the infectious period (see below), and the indirect transmission can be modeled, to good approximation, as a transmission through direct contact. The amount of local ground contamination depends on the spatial behaviour of the mouse, and therefore the ground contamination will have the same distribution as the mouse probability distribution function, i.e., it is proportional to $K_a(\vec{r})$.

In the model, the β-value captures the virus transmission coefficient, be it direct or indirect via ground contamination. This value is unknown, but we estimated this phenomenological variable using the observations of Borremans et al. (2011). They observed antibody prevalences of Mopeia virus of 13% for populations of *M. natalensis* in Tanzania in the dispersal season. We ran the simulations for a range of β-values, and chose $\beta = 125\ m^2/\text{mouse/day}$, as this value resulted in an antibody

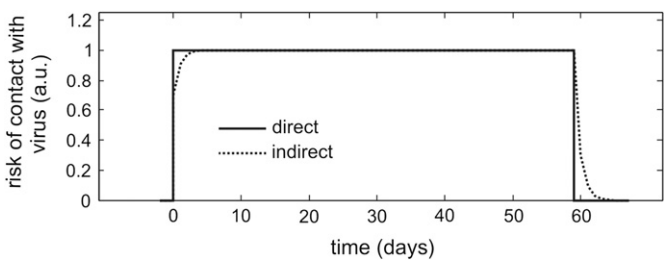

Fig. 1. The risk of contact with virus from one infectious neighbour via direct contact (solid line) or indirect contact (dotted line).

prevalence of 13% in the dispersal season. Because this is still a rough estimate, β will be examined in a sensitivity analysis.

Note that, when calculated on a grid, the current approach with the Gaussian kernel speeds up the calculation significantly, since the calculation of the infection rate (matrix ψ), is in fact a convolution of the matrix of the number of infected mice in each of the grid cells, $N_i(\overrightarrow{r})$, with the above overlap function, see Eq. (5), i.e., a two dimensional Gaussian kernel. The determining factor for the grid size is the width of the overlap function: the grid size should be small enough to capture the Gaussian shape. Therefore, in the simulations, a grid size of 5 m($<\sqrt{2}\sigma$) was used.

E→I

After an experimental infection of guinea pigs with Lassa virus, virus titers reached a more or less constant phase around day 7 after inoculation in salivary glands, kidney and lungs (Jahrling et al., 1982). Since these organs are probable to be responsible for the virus shedding (in salivation, urine, and aerosols), we use an average exposed (latent) period of 7 days, which corresponds to a transition rate of $\xi = 0.14$ mice/day.

I→R

In the infection experiments of Walker et al. (1975) on *M. natalensis*, Lassa virus disappeared from the liver between days 12 and 29, from the lungs between days 29 and 58 and from the spleen between days 58 and 103. Lacking specific data for Mopeia virus, we assume a similar average infectious period of 60 days, resulting in a transition rate $\gamma = 0.017$ mice/day.

A list of all the parameters used in the model is given in Table 1.

2.4. Simulation setup

Every simulation is started at the end of the reproductive season, with a population size equal to the carrying capacity. The individuals are distributed randomly on a square grid. In the middle of the first dispersal season, the infection is introduced in the population by infecting a single individual in the center of the patch. This is the most likely time for (infected) individuals to immigrate the patch, but another introduction moment would not alter the long term persistence or infection dynamics after invasion. The simulation is then run until the infection fades out, with a maximum simulation time of 10 years. Each simulation was run 6000 times or more, until stochastic fluctuations became small.

2.5. Invasion and persistence

Because of the strong annual seasonality of *M. natalensis*, and for easy interpretation, virus presence is inspected in discrete time steps of 1 year. For every year t, we calculate, from the ensemble of simulations, the probability that the infection survives until the next year $t+1$, which we denote as $p(t+1|t)$ (note that we consider the survival of the infection, not of single viruses). The probability for the infection to exist at year T, is then given by

$$p(T) = \prod_{t=0}^{t=T-1} p(t+1|t). \tag{7}$$

This annual survival probability $p(t+1|t)$ of the infection will change over time. Indeed, immediately after the initial infection, the infection survival probability is very much determined by this initial condition, i.e., the fact that the infection is limited in size, localized in the center of the patch. As time goes by and the infection does not disappear, it will spread to more distant parts of the patch, and consequently, the effects of the initial boundary condition are lifted, so that, eventually, the probability for the infection to survive no longer changes over time. We will study the dynamics of this varying annual survival probability and make a rough distinction between invasion and persistence. The invasion probability is the probability $p_I = p(1|0)$ that the infection survives the first year in the population, i.e., this initial infection succeeded in invading the population. The persistence probability p_P is the probability that the infection, after invading and spreading throughout the patch, persists until the next year. In this case, the annual survival probability has converged to a fixed value $p_P = \lim_{t\to\infty} p(t+1|t)$.

In case the virus has successfully invaded the population ($p_I = 1$), the above equation can be approximated by

$$p(T) \approx p_P^T \tag{8}$$

$$p(T) = e^{\log(p_P)\cdot T}, \tag{9}$$

and consequently, the mean duration of persistence is then given by $T_P = -1/[\log(p_P)]$.

3. Results

3.1. Course of infection

The typical course of a Mopeia virus infection is shown in Fig. 2 for a single simulation. In the reproductive season, the number of newly infected mice (E) increases. Subsequently, also the number of infectious individuals (I) increases. After the reproductive period, the number of infected mice decreases until the start of the dispersal season. In this dispersal season there is a second peak in the number of infected mice. The maximum number of infected mice is usually smaller than in the reproductive period, but, because of the lower population size, the antibody prevalence is still high. Sometimes, the persistence of the infection depends on only very few infected mice. This is for example the case around day 2000 in Fig. 2.

Table 1
List of the parameters used in the simulations.

	Parameter	Symbol	Value
Demographic component	Birth rate	v	0.031 mice/day
	Death rate below carrying capacity	μ	0.0073 mice/day
	Death rate above carrying capacity	μ	0.0111 mice/day
	Litter size		11 mice
Spatial component	Length grid cell		5 m
	Radius home range		14.3 m
	Dispersal distance	d	300 m
	Monthly dispersal percentage in the dispersal season	f	24%
Infection component	Rate of E–I transition	ξ	0.14 mice/day
	Rate of I–R transition	γ	0.017 mice/day
	Transmission coefficient	β	125 m^2/mouse/day

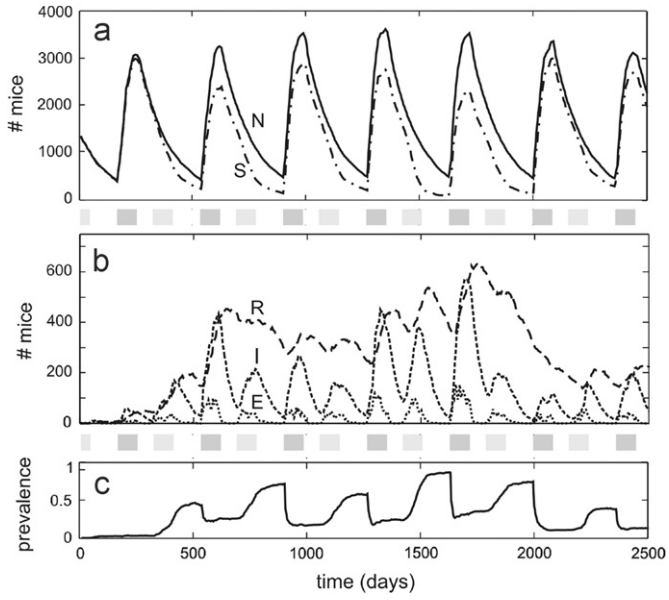

Fig. 2. The results for a single simulation of a patch of 30 ha with a carrying capacity of 100 mice/ha. The number of susceptibles and total population size are shown at the top (a). In the middle (b) the numbers of mice in the latent, infectious and recovered stage are shown. The prevalence of mice with antibodies (in the infectious or recovered phase) is shown at the bottom (c). The reproductive seasons are indicated in dark grey, the dispersal periods in light grey.

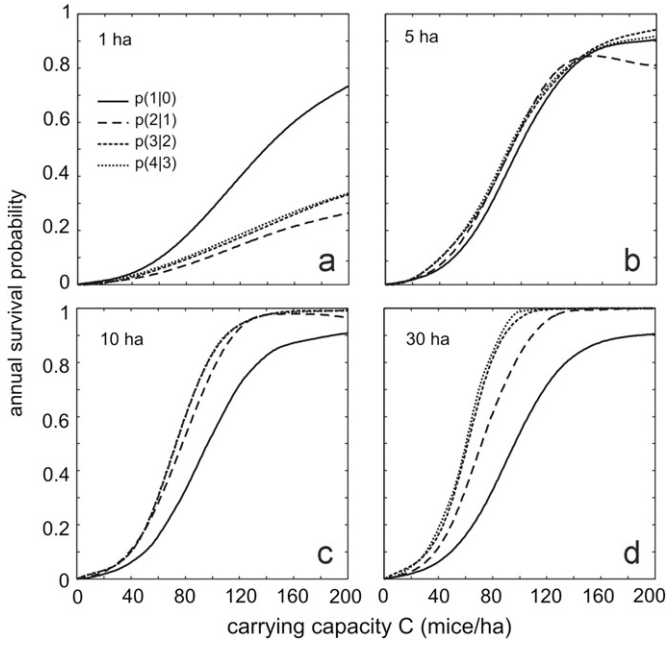

Fig. 3. The annual survival probability $p(t+1|t)$ is plotted as a function of the carrying capacity C, for patch sizes of 1, 5, 10 and 30 ha. The results are shown for the first 4 years of the simulations.

3.2. Annual survival probability

The annual survival probability, $p(t+1|t)$, is shown in Fig. 3 for patch sizes of 1, 5, 10 and 30 ha. The carrying capacity in our model ranges between 5 and 200 mice/ha. In reality, even higher population densities are observed (Leirs et al., 1997). Only the data of the first 4 years are shown.

For the invasion probability $p_I = p(1|0)$, it is clear that p_I increases as a function of the carrying capacity C for all patch sizes. The invasion probability p_I is lowest in case of the 1 ha patch, increases with increasing patch size, to converge already at a patch size of 10 ha. Indeed, the invasion probability curves are identical in Fig. 3(c) and (d).

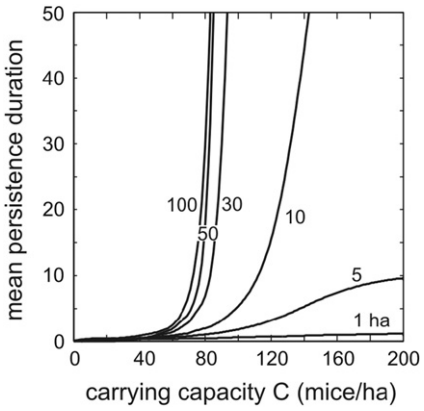

Fig. 4. The mean duration of persistence is plotted as a function of the carrying capacity C for patches of 1, 5, 10, 30, 50 and 100 ha.

The probability to survive year $t=1, 2, 3$ also increases with increasing carrying capacity C, apart from $p(2|1)$ in Fig. 3(b) and (c). For the 5 and 10 ha patch sizes, for higher C-values, $p(2|1)$ decreases for increasing C. $p(2|1)$ is well below the invasion probability curve in case of the 1 ha patch; for the other patches, the opposite is true and $p(2|1) > p(1|0)$. The annual survival probability increases with increasing t, to converge at the persistence probability p_P. The larger the patch, the higher p_P and the longer it takes to converge.

3.3. Mean duration of persistence

In Fig. 4, the mean duration of persistence (or mean time to fade out) T_P is plotted as a function of the carrying capacity for patch sizes of 1, 5, 10, 30, 50 and 100 ha. The mean duration of persistence increases with increasing C, but in a patch of 1 ha, T_P is always very low (lower than 1 year). As the patch size increases, T_P increases, especially for higher C-values, and the larger the patch, the more persistence is governed by a threshold based on the carrying capacity C.

3.4. Sensitivity analysis

Because the model parameters are not known precisely, the sensitivity of the invasion and persistence probabilities to the transmission coefficient β, the transition rates ξ and γ, the monthly dispersal rate f, the dispersal distance d and the home range kernel σ are tested. The results are shown in Fig. 5 for patches of 1 ha (a, b) and 30 ha (c, d). Each of these parameters is increased separately by 30% and 12 000 simulations are run in which the infection is still present after the first year. The results show that the I–R transition rate γ has a large effect on invasion and persistence, in both patch sizes: a shorter infectious phase $(1/\gamma)$ leads to a lower annual survival probability of the infection. The home range kernel σ has an equally large (but positive) effect, except during persistence in the 1 ha patch. At high carrying capacities, a larger home range has a small negative effect on persistence probability in the smallest patch. A 30% increase of the transmission coefficient β increases the annual survival probability during invasion, while it has no influence during persistence. The same increase of ξ only causes a minor increase in annual survival probability during invasion in the 30 ha patch. Increases in the dispersal rate f or the dispersal distance d do not change the annual survival probability, during invasion nor during persistence in either of the patch sizes.

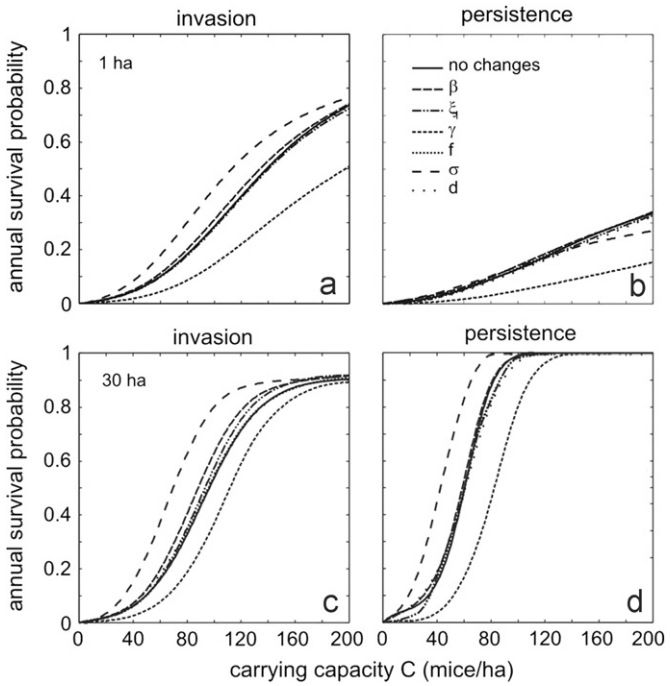

Fig. 5. The annual survival probability during invasion and persistence is plotted as a function of the carrying capacity C for the model without changes as well as for models with a 30% increase in the transmission coefficient β, E–I transition rate ξ, I–R transition rate γ and monthly dispersal percentage f, dispersal distance d and the home range kernel σ. The simulated patch sizes are 1 ha (a, b) and 30 ha (c, d).

4. Discussion

The pattern that comes out of the model most clearly, is that each year two infection waves occur. The first wave, during and right after the reproductive season, can be explained by the inflow of newborns. This enhances the infection spreading in two ways: through an increase in the number of susceptible hosts and through a higher host density, enhancing transmission. After this wave, the number of infected animals again decreases because of a local depletion of susceptible animals. During the dispersal period, the second wave follows as a result of the movement of infected hosts away from sites where susceptible animals are depleted locally, to areas where the proportion of susceptibles is higher due to the absence of infection or the disappearance of previous infections. This effect of host movement on seasonality and spread of infectious diseases was also found by Grassly and Fraser (2006) and White et al. (2000). Indeed, dispersal is an important process for infection spread and persistence, and Jesse and Heesterbeek (2011) showed that its effect depends on the distance hosts disperse. Because the population is already decreasing during the second infection wave, the infection prevalence is highest during this period. Such a relationship between density and prevalence was not found in an empirical study about Lassa virus in Guinea (Fichet-Calvet et al., 2008). However, these West African *M. natalensis* populations only fluctuate slightly (factor two at most, Fichet-Calvet et al., 2008), while in East Africa, population fluctuations from 20 to 500 multimammate mice per hectare within a couple of months are common (Leirs et al., 1997; Sluydts et al., 2007).

The invasion probability rises with increasing carrying capacities. This can be attributed to the density dependent nature of the virus transmission (Davis et al., 2005). As more mice can be sustained on patches with a higher carrying capacity, infected animals are more likely to encounter a susceptible animal, which increases the spreading potential of the virus. There is however an important influence of patch size. In small patches (e.g. 1 ha, Fig. 3) the invasion probability is lower than in larger patches due to a depletion of susceptible animals, causing the infection to disappear more easily. In contrast, in larger patches (>5 ha) the invasion probability is rather independent of the patch size, because the number of susceptible animals does not become low enough to hamper transmission.

In general, the survival probability of an infection in the second year (after a successful invasion) is higher than during the invasion period (Fig. 3(b), (c)), and increases even further in the following years for big patches (≥ 30 ha). This can be explained by the higher number of infectious animals at the start of the second year compared to the first year, which increases the probability of successfully transmitting the infection. This process continues for several years in larger patches (≥ 30 ha), because the yearly travel distance of the infection is limited. For the smallest patches however, this reasoning no longer holds, because the proportion of immune (recovered) individuals becomes too high, which causes the population to reach a state of herd immunity, and therefore the probability for the infection to disappear increases after the first year (Fig. 3(a)). The same holds for medium sized patches when the virus is transmitted exceptionally rapid during the first reproductive season because of high carrying capacities (Fig. 3(b), (c)). This causes a lack of susceptible (and infectious) mice at the beginning of the second year, which we observe as a decline of $p(2|1)$ at high C in Fig. 3(b) and (c). In later years, the new infections are spread more evenly throughout the year, so the annual survival probability stabilizes.

Theoretical compartmental models using coupled differential equations and assuming random mixing clearly show abrupt thresholds at $R_0 = 1$ (the basic reproductive ratio, Heesterbeek, 2002). Hence, due to the density dependent nature of the virus transmission, classical theory predicts abrupt threshold behaviour as a function of the carrying capacity. When trying to use more realistic models however (stochastic and non-random mixing as in our case), it is known that such thresholds can get strongly blurred (Lloyd-Smith et al., 2005), which makes it more difficult to define a threshold and to prove its presence. (Indeed, the 'abruptness' of a threshold is always relative to the dynamic range of the independent variable, in this case, to the changes of the carrying capacity that occur in the field). Therefore, in our case, we do not see abrupt thresholds. In case of invasion – which is particularly prone to stochasticity due to the limited number of initially infected – there is no abrupt threshold, but rather a continuous transition. In case of persistence, threshold behaviour is more apparent for larger patch sizes (10 and 30 ha): we see a steep increase in the persistence probability within a limited density range (of about 60 and 110 animals/ha in the 10 ha patch and about 40 and 90 animals/ha in the 30 ha patch (Fig. 3)). For the smaller patches, this pattern – a steep increase of the persistence probability – is less obvious (5 ha) or seems to totally disappear (1 ha).

So far, we have looked at thresholds on the survival probability at the 1-year level, but thresholds manifest themselves more clearly on longer timescales. Indeed, the probability to persist for a certain period of time will be a steeper function of the carrying capacity (and hence more threshold-like) as the time to persist increases. For this reason, it is useful to study the infection dynamics on a longer time scale, and therefore, we look at the mean duration of persistence (or the mean time to fade out), which can be derived from the persistence probability. Here, the threshold behaviour for patch sizes above 10 ha, which was already visible in the persistence probability curve, is more distinct, with a threshold carrying capacity somewhere between 70 and 90 animals/ha.

The sensitivity analysis shows that the role of the transmission parameters is not the same for invasion and persistence. The invasion probability is more sensitive to the transmission coefficient β,

compared to the persistence probability. A higher rate of virus transmission increases the likelihood of surviving the first year, but as soon as the infection has successfully settled in a population, the infection is less sensitive to changes in the transmission coefficient. The 30% change of the latent period does not have a strong influence on persistence probability, although the invasion probability in the 30 ha patch is slightly higher for shorter latent periods. The shorter the latent period, the faster the infection will spread, which is especially beneficial for infection survival in the first year. For persistence in the following years, this is of less importance, because the infection is well established in the patch, and there are more infected animals that can spread the virus. The infectious period does have a strong influence, for invasion as well as persistence in both patch sizes. A shorter infectious period strongly decreases the invasion and persistence probabilities, because infected individuals can infect less animals, thereby increasing the probability of infection fade-out. An increased home range on the other hand strongly increases the possible number of contacts between animals, resulting in an increased invasion probability in both patch sizes. In the 30 ha patch, a larger home range has the same positive effect on persistence probability, while in the 1 ha patch it only has a small negative effect at the highest carrying capacities. The latter is due to the same mechanism described earlier to explain the role of patch size: a larger home range creates infection opportunities for a higher number of animals, thereby increasing the proportion of recovered mice, which in turn decreases the persistence probability (herd immunity) in very small patches. The monthly dispersal percentage does not seem to significantly change the annual survival probability. Although dispersion obviously influences the number of infections (Fig. 2), a 30% increase in the number of dispersing hosts barely changes the invasion or persistence capacity. In other words, a low percentage of dispersing hosts positively influences transmission, while it seems that as soon as a sufficient number of hosts disperse, a further increase in the number of dispersing animals does not necessarily result in a higher invasion or persistence probability. The same is true for dispersal distance: as long as the distance is larger than the minimum distance needed to reach new areas containing susceptibles, dispersal distance does not strongly influence invasion and persistence probabilities.

Aside from investigating the existence and nature of abundance thresholds, the purpose of this simulation model was the identification of parameters that exert a strong influence on transmission. The findings of our model, i.e. the importance of the infectious period and the transmission coefficient, and the possible existence of abundance thresholds, can guide future and ongoing experimental studies on Mopeia virus transmission. Taking the extensive existing knowledge on the population dynamics of its host into account, our results suggest that the Mopeia virus-multimammate mouse system can be of high value for thoroughly understanding the transmission of a rodent-borne infection, and in particular for testing hypotheses regarding the role of population density for virus invasion and persistence.

References

Abramson, G., Giuggioli, L., Kenkre, V., Dragoo, J., Parmenter, R., Parmenter, C., Yates, T., 2006. Diffusion and home range parameters for rodents: *Peromyscus maniculatus* in New Mexico. Ecol. Complexity 3, 64–70.

Bartlett, M., 1960. The critical community size for measles in the United States. J. R. Stat. Soc. Ser. A 123, 37–44.

Begon, M., Bennett, M., Bowers, R., French, N., Hazel, S., Turner, J., 2002. A clarification of transmission terms in host-microparasite models: numbers, densities and areas. Epidemiol. Infect. 129, 147–153.

Borremans, B., Leirs, H., Gryseels, S., Günther, S., Makundi, R., Goüy de Bellocq, J., 2011. Presence of Mopeia virus, an African arenavirus, related to biotope and individual rodent host characteristics: implications for virus transmission. Vector-Borne Zoonotic Dis. 11, 1125–1131.

Davis, S., Begon, M., De Bruyn, L., Ageyev, V., Klassovskiy, N., Pole, S., Viljegrein, H., Stenseth, N., Leirs, H., 2004. Predictive thresholds for plague in Kazakhstan. Science 304, 736–738.

Davis, S., Calvet, E., Leirs, H., 2005. Fluctuating rodent populations and risk to humans from rodent-borne zoonoses. Vector-Borne Zoonotic Dis. 5, 305–314.

Deredec, A., Courchamp, R., 2003. Extinction thresholds in host-parasite dynamics. Ann. Zool. Fenn. 40, 115–130.

Fichet-Calvet, E., Lecompte, E., Koivogui, L., Daffis, S., Ter Meulen, J., 2008. Reproductive characteristics of *Mastomys natalensis* and Lassa virus prevalence in guinea West Africa. Vector-Borne Zoonotic Dis. 8, 41–48.

Grassly, N., Fraser, C., 2006. Seasonal infectious disease epidemiology. Proc. R. Soc. B 273, 2541–2550.

Günther, S., Lenz, O., 2004. Lassa virus. Crit. Rev. Clin. Lab. Sci. 41, 339–390.

Heesterbeek, J., 2002. A brief history of R_0 and a recipe for its calculation. Acta Biotheor. 50, 189–204.

Jahrling, P., Smith, S., Hesse, R., Rhoderick, J., 1982. Pathogenesis of Lassa virus infection in guinea pigs. Infect. Immun. 37, 771–778.

Jay, M., Glaser, C., Fulhorst, C., 2005. The arenaviruses. J. Am. Vet. Med. Assoc. 227, 904–915.

Jesse, M., Heesterbeek, H., 2011. Divide and conquer? Persistence of infectious agents in spatial metapopulations of hosts. J. Theor. Biol. 275, 12–20.

Keeling, M., Rohani, P., 2007. Modeling Infectious Diseases in Humans and Animals. Princeton University Press.

Kermack, W., McKendrick, A., 1927. A contribution to the mathematical theory of epidemics. Proc. R. Soc. London A 115, 700–721.

Leirs, H., 1994. Population ecology of *Mastomys natalensis* (Smith 1834). Implications for rodent control in Africa: a report from the Tanzania–Belgium joint rodent research project (1986–1989). Agricultural edition, Belgian administration for development cooperation.

Leirs, H., Stenseth, N., Nichols, J., Hines, J., Verhagen, R., Verheyen, W., 1997. Stochastic seasonality and nonlinear density-dependent factors regulate population size in an African rodent. Nature 389, 176–180.

Leirs, H., Verhagen, R., Verheyen, W., 1993. Productivity of different generations in a population of *Mastomys natalensis* rats in Tanzania. Oikos 68, 53–60.

Leirs, H., Verheyen, W., Verhagen, R., 1996. Spatial patterns in *Mastomys natalenis* in Tanzania (Rodentia, Muridae). Mammalia 60, 546–555.

Lloyd-Smith, J., Cross, P., Briggs, C., Daugherty, M., Getz, W., Latto, J., Sanchez, M., Smith, A., Swei, A., 2005. Should we expect population thresholds for wildlife disease. Trends Ecol. Evol. 20, 511–519.

Lloyd-Smith, J., Wayne, M., Westerhoff, H., 2004. Frequency-dependent incidence in models of sexually transmitted diseases: portrayal of pair-based transmission and effects of illness on contact behaviour. Proc. R. Soc. London B 271, 625–635.

Monadjem, A., Perrin, M., 1998. The effect of supplementary food on the home range of the multimammate mouse *Mastomys natalensis*. S. Afr. J. Wildl. Res. 28, 347–356.

Nåsell, I., 2005. A new look at the critical community size for childhood infections. Theor. Popul. Biol. 67, 203–216.

Peters, C., Jahrling, P., Kenyon, R., McKee, K., Oro, J., 1987. Experimental studies of arenaviral hemorrhagic fevers. Curr. Top. Microbiol. Immunol. 134, 5–68.

Sagripanti, J.L., Rom, A., Holland, L., 2010. Persistence in darkness of virulent alphaviruses, Ebola virus, and Lassa virus deposited on solid surfaces. Arch. Virol. 155, 2035–2039.

Seaman, D., Powell, R., 1996. An evaluation of the accuracy of kernel density estimators for home range analysis. Ecology 77, 2075–2085.

Shchipanov, N., Lyapina, M., 2008. Home range and the expression of nonresidence in bank voles (*Clethrionomys glareolus*): interpretation of the results of marking at live-trap lines. Russ. J. Ecol. 39, 359–365.

Sluydts, V., Crespin, L., Davis, S., Lima, M., Leirs, H., 2007. Survival and maturation rates of the African rodent, *Mastomys natalensis*: density-dependence and rainfall. Integrative Zool. 2, 220–232.

Van Hooft, P., Cosson, J., Vibe-Petersen, S., Leirs, H., 2008. Dispersal in *Mastomys natalensis* mice: use of fine-scale genetic analyses for pest management. Hereditas 145, 262–273.

Veenstra, A., 1957. The behaviour of the multimammate mouse, Rattus (Mastomys) natalensis (A. Smith). Anim. Behav. 6, 192–206.

Walker, D., Wulff, H., Lange, J., Murphy, F., 1975. Comparative pathology of Lassa virus infection in monkeys, guinea-pigs, and *Mastomys natalensis*. Bull. World Health Org. 52, 523–534.

White, A., Watt, A., Hails, R., Hartley, S., 2000. Patterns of spread in insect–pathogen systems: the importance of pathogen dispersal. Oikos 89, 137–145.

Wilkinson, D., 2006. Stochastic Modelling for Systems Biology. Chapman and Hall/CRC.

Worton, B., 1989. Kernel methods for estimating the utilization distribution in home-range studies. Ecology 70, 164–168.